Journal of Southeast University (English Edition) Vol. 29, No. 4, pp. 419 - 424 Dec. 2013 ISSN 1003—7985

Aerodynamics of flexible wing in bees' hovering flight

Yin Dongfu Zhang Zhisheng

(School of Mechanical Engineering, Southeast University, Nanjing 211189, China)

Abstract: The aerodynamics of 2-dimensional flexible wings in bees' normal hovering flight is studied. Four insect flapping flight coordinate systems, including a global system, a body-fixed system, a rigid wing-fixed system and a flexible wing-fixed system, are established to represent the insects' position, gesture, wing movement and wing deformation, respectively. Then the transformations among four coordinate systems are studied. It is found that the elliptic coordinate system can improve the computation accuracy and reduce the calculation complexity in a 2-dimensional rigid wing. The computation model of a 2-dimensional flexible wing is established, and the changes of the force, moment, and power are investigated. According to the computation results, the large lift and drag peaks at the beginning and end of the stroke can be explained by the superposition of the rapid translational acceleration, the fast pitching-up rotation and the Magnus effect; and the small force and drag peaks can be explained by the convex flow effect and the concave flow effect. Compared with the pressure force, pressure moment and translational power, the viscous force, viscous moment and rotational power are small and can be ignored.

Key words: flapping wing; coordinate systems; hovering flight; computational fluid dynamics; aerodynamics force; power

doi: 10.3969/j.issn.1003-7985.2013.04.012

Humans have long been fascinated with flight through the air, and observations of nature fliers' effortless defiance of gravity first inspired our dreams of taking to the air. Nonetheless, the early attempts to use flapping wings for propulsion failed; consequently, researchers paid more attention to fixed and rotary wings study and achieved great success in the past 100 years. However, traditional fixed-wing and rotary-wing flight began to fail as the flow dynamics entered a regime of insect-sized flights. The small scale air vehicles require different design ideas compared with the conventional ones. Then researchers turned to micro air vehicle (MAV) design by imitating insect flight, and looked forward to producing the micro flapping vehicle. But we have less-detailed understanding of flight mechanics so far. Previous studies show that the steady-state mechanism is inadequate to predict the aerodynamic lift and power requirements of small insects[1]. Some new techniques, such as the computational fluid dynamics (CFD) method and the unsteady theory, are required to reveal the mechanism of insect flight.

Previous studies on flapping flight have been undertaken from analytical, experimental and computational aspects. Sun et al.[2] investigated lift and power requirements for hovering flight in Drosophila virilis using the computational fluid dynamics method. Wang et al.[3] compared computational, experimental and quasi-steady forces in a generic hovering wing undergoing sinusoidal motion along a horizontal stroke plane. Liu[4] addressed an integrated and rigorous model for the simulation of insect flapping flight. However, the above models are based on idealized rigid wings and they do not consider the effect of the wings' flexion during insect hovering flight. Insects use flapping wings to generate forces to balance their weight for hovering. Although insect wings are small and only account for 0.4% to 6.0% of body mass, they provide enough force for insect flight[5]. For the lift coefficient, the moderate wing flexibility leads to a 15% to 30% increase compared with the rigid wing[6]. To understand the mechanism of insect flight, Tanaka et al.[5,7] investigated wing flexibility on lift generation in hoverfly flight, and they pointed out that the flexible deformation should not be ignored.

In order to hovering, the flapping wings need to generate enough lift to support body weight in the vertical direction while maintaining a balance of aerodynamic forces and moments to stabilize the body, and need to consume more power compared with forward flight[8]. To provide a detailed view of the aerodynamics, control and energetics of the flexible wing in insect normal hovering flight, the aerodynamics of 2-dimensional flexible wing in bees' hovering flight is studied. Understanding the mechanism of insect flight will help us to design micro-flapping flight aircraft.

1 Insect Flapping Flight Coordinate Systems

1.1 Four coordinate systems of flapping flight

To study the movement and deformation of the insect wings, four coordinate systems are defined as follows[4]:

1) A global system ($o_0x_0y_0z_0$) It is equivalent to an

Received 2013-07-19.

Biographies: Yin Dongfu (1986—), male, graduate; Zhang Zhisheng (corresponding author), male, doctor, professor, oldbc@seu.edu.cn.

Foundation items: The Fundamental Research Funds for the Central Universities (No. 3202003905), Scientific Innovation Research of College Graduates in Jiangsu Province (No. CXLX12_0080).

Citation: Yin Dongfu, Zhang Zhisheng. Aerodynamics of flexible wing in bees' hovering flight[J]. Journal of Southeast University (English Edition), 2013, 29(4): 419 - 424. [doi: 10.3969/j.issn.1003 - 7985.2013.04.012]

inertial system.

2) A body-fixed system ($o_1x_1y_1z_1$) Its origin is in the centroid of an insect, positive x_1 oriented the insect head, positive z_1 oriented the wing tip, positive y_1 oriented vertically upward. Fig. 1(a) shows the angles of pitch θ, roll φ, and yaw ψ with respect to the body-fixed system.

3) A rigid wing-fixed system ($o_2x_2y_2z_2$) Its origin is at the root of the insect wings. The wing root is coinciding with the insect centroid, positive x_2 oriented the leading edge, positive z_2 oriented the wing tip, positive y_2 oriented vertically upward. Fig. 1(b) shows the positional angle ξ, the elevation angle $\tilde{\varepsilon}$, and the angle of attack α with respect to the rigid body-fixed system.

4) A flexible wing-fixed system ($o_3x_3y_3z_3$) Its origin is at the centroid of the insect wings, positive x_3 oriented the leading edge, positive z_3 oriented the wing tip, positive y_3 oriented vertically upward.

The deformation of the insect wings generally includes chordwise and spanwise deflections[6], so the chordwise bending angle δ and the spanwise bending angle γ are defined. The wing near root and leading edge is simplified as rigid and the other part is flexible. Fig. 1(c) shows the chordwise bending angle δ and the spanwise bending angle γ with respect to the flexible body-fixed system.

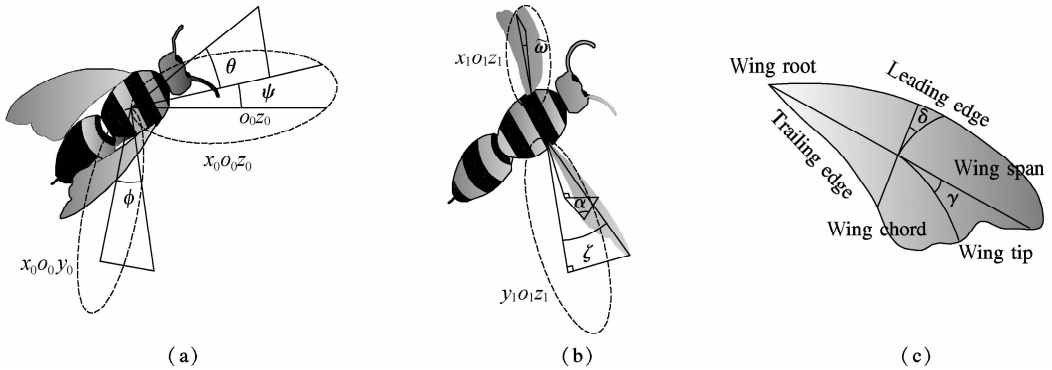

Fig. 1 Definition of insect flapping angles. (a) Body-fixed coordinate System; (b) Rigid wing-fixed coordinate system; (c) Flexible wing-fixed coordinate system

1.2 Transformation among four coordinate systems

The global system, the body-fixed system, the rigid wing-fixed system and the flexible wing-fixed system are used to reveal the insects' position, gesture, the wings movement, and the wings deformation, respectively. To solve the general problem of insect flight, the coordinate system transformation is investigated. As shown in Fig. 2(a), the transformation between the global system and the body-fixed system can be written as

$$\boldsymbol{S}_{\theta\psi j}=\begin{bmatrix}\cos\psi\cos\theta & \cos\psi\sin\theta & -\sin\psi\\ \sin\varphi\sin\psi\cos\theta-\cos\varphi\sin\theta & \sin\varphi\sin\theta\sin\psi+\cos\varphi\cos\theta & \sin\varphi\cos\psi\\ \cos\varphi\sin\psi\cos\theta+\sin\varphi\sin\theta & \cos\varphi\sin\theta\sin\psi-\sin\varphi\cos\theta & \cos\varphi\cos\psi\end{bmatrix} \tag{1}$$

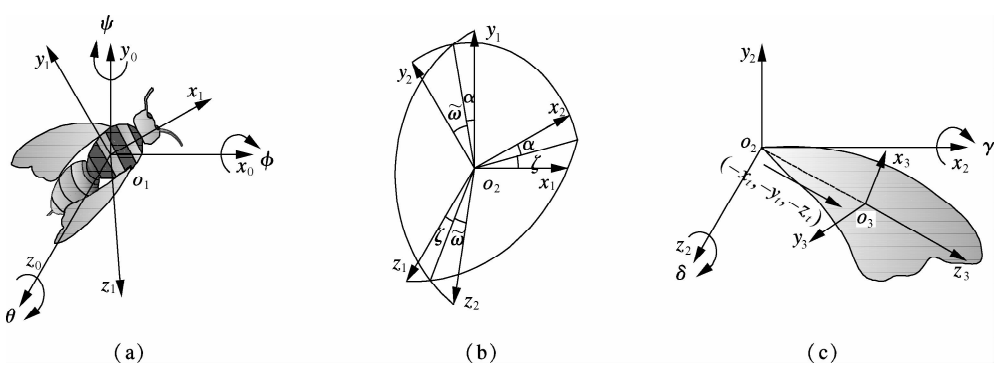

Fig. 2 Transformation among four coordinate systems. (a) Transformation between global system and body-fixed system; (b) Transformation between body-fixed system and rigid wing-fixed system; (c) Transformation between rigid wing-fixed system and flexible wing-fixed system

As shown in Fig. 2(b), the transformation between the body-fixed system and the rigid wing-fixed system can be written as

$$\boldsymbol{S}_{\alpha\zeta\tilde{\omega}}=\begin{bmatrix}\cos\alpha\cos\zeta & \cos\zeta\sin\alpha & -\sin\zeta\\ \sin\tilde{\omega}\sin\zeta\cos\alpha-\cos\tilde{\omega}\sin\alpha & \cos\tilde{\omega}\cos\alpha+\sin\tilde{\omega}\sin\alpha\sin\zeta & \sin\tilde{\omega}\cos\zeta\\ \sin\tilde{\omega}\sin\alpha+\cos\tilde{\omega}\sin\zeta\cos\alpha & \cos\tilde{\omega}\sin\alpha\sin\zeta-\sin\tilde{\omega}\cos\alpha & \cos\tilde{\omega}\cos\zeta\end{bmatrix} \tag{2}$$

As shown in Fig. 2(c), the transformation between the rigid wing-fixed system and the flexible wing-fixed system can be written as

$$\boldsymbol{S}_{\delta\gamma\boldsymbol{K}}=\begin{bmatrix}\cos\delta & \sin\delta & 0 & 0\\ -\cos\gamma\sin\delta & \cos\gamma\cos\delta & \sin\gamma & 0\\ \sin\gamma\sin\delta & -\sin\gamma\cos\delta & \cos\gamma & 0\\ -x' & -y' & -z' & 1\end{bmatrix} \quad (3)$$

where $\boldsymbol{K}=(-x_t,\ -y_t,\ -z_t)$, and $\boldsymbol{K}$ is a vector pointing from o_2 to o_3.

1.3 Elliptic coordinate system

Although the above coordinate systems have the versatility, the elliptic coordinate system may be more helpful in 2-dimensional wing research. The computation of 2-dimensional insect hovering showed that a hovering motion can generate enough lift to support a typical insect weight[9]. As the cross-section of 2-dimensional wings is similar to an ellipse, wing chord can be simplified as an ellipse to facilitate the theoretical analysis and computation. The movement of the ellipse can be expressed in the elliptical coordinate. Fig. 3 shows the established elliptic coordinate system.

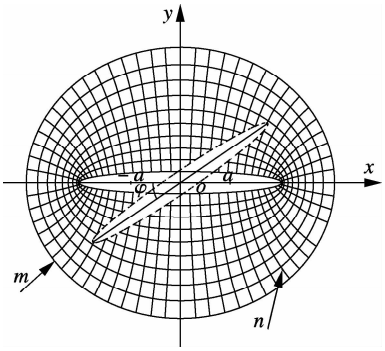

Fig. 3 Established elliptic coordinate system

The conversion between the elliptic coordinate system and the Cartesian coordinate system is

$$x=a\cosh m\cos n,\quad y=a\sinh m\sin n \quad (4)$$

where $(-a,\ 0)$ and $(a,\ 0)$ are two focuses of the ellipse; curves of constant m form ellipses, and curves of constant n form hyperbolae. The dashed ellipse represents the torsional wing chord and φ is the torsion angle. The center of the ellipse coordinate system coincides with the center of the wings' cross-section. The Navier-Stokes equation and the continuity equation expressed in the elliptic coordinate system have the following forms[10]:

$$\frac{\partial(S\boldsymbol{w})}{\partial t}+(\sqrt{S}\boldsymbol{u}\cdot\nabla)\boldsymbol{w}=v\Delta\boldsymbol{w},\quad \nabla\sqrt{S}\boldsymbol{u}=0 \quad (5)$$

where $\boldsymbol{u}$ is the velocity field; $\boldsymbol{w}$ is the vorticity field; v is the velocity and S is the scaling factor. The mesh points are naturally clustered around the tips in the elliptical coordinate system. The radius of the computational boundary can be chosen to be 5 to 10 times the half-chord length[3]. While in the Cartesian coordinate system, this value is 20 to 50 times the half-chord length, so it can improve the computational accuracy and reduce the calculation complexity.

2 Computation Models and Methods

Fig. 4(a) shows the forces and position of a rigid wing in the downstroke phase. During the hovering flight, the tip angle of the stroke plane is particularly small and the stroke plane is approximately horizontal. Hovering with a horizontal stroke plane is termed normal hovering[11]. The wing deformation of normal hovering flight can be represented as Fig. 4(b). The thick line represents the wing chord and the filled circle represents the leading edge. In Fig. 4, α is the angle of attack; φ is the torsion angle; $\boldsymbol{F}_{\mathrm{L}}$ is the lift and $\boldsymbol{F}_{\mathrm{D}}$ is the drag. In hovering flight, $\boldsymbol{F}_{\mathrm{D}}$ is equal to thrust in the horizontal direction and $\boldsymbol{F}_{\mathrm{L}}$ is equal to the insect weight in the vertical direction. Insect wings have two forms of movements in one flapping cycle; the wing chord will distort at the beginning and end stage and translate at the middle stage in the stroke plane. The translational movement of a wing is governed by $A(t)=A_0/2\ [\cos(2\pi t/T)+1]$, and the rotational movement is governed by $a(t)=\pi/[4(1-\sin(2\pi t/T))]$[12]. Other wing flexure deformation parameters are set the same values as those in Ref. [13].

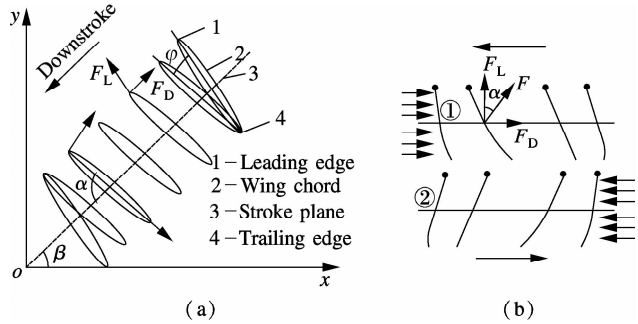

Fig. 4 The generated forces and movement of wings. (a) Rigid wings in forward flight; (b) Flexible wings in hovering flight

The computational fluid dynamics problem is defined under the initial and boundary conditions. The solutions to the N-S equations require specific boundary conditions at the solid walls of dynamic flapping wings and the body as well as at the far-field outside boundary. The computational domain has a size of $50c\times 50c$, where c is the length of the wing chord. Extensive tests have been done to make sure that the domain is large enough to achieve satisfactory accuracy of the results. The outermost boundary of the computational domain is defined as the pressure-outlet wall. The wing boundary condition satisfies $v_{t=0}=0$ at the initial movement. The fluid velocity at fluid-wing boundaries is equal to that of the wing boundary.

The no-slip condition for viscous fluids states that at the wing boundary, it satisfies the condition $v_{\text{fluid}} = v_{\text{wing}}$.

The second-order up-wind numerical scheme and the SIMPLEC algorithm are used to solve 2-dimensional incompressible Navier-Stokes equations. At each time step, user-defined functions (UDFs) are used to control the wing's motions and to obtain the aerodynamic performance. Dynamic mesh techniques are implemented by using the spring-based smoothing model and the local remeshing model.

The process to calculate the force, moment and power is as follows:

1) The pressure distribution of every face thread is obtained first, and then the pressure force is computed by looping over all face threads in the domain. The total force is the cumulative force of each face. In hovering flight, lift is the component of total force in the vertical direction, $\boldsymbol{F}_{\text{L}} = \boldsymbol{F}\cos\alpha$, and drag is the component of total force in the horizontal direction, $\boldsymbol{F}_{\text{D}} = \boldsymbol{F}\sin\alpha$ (see Fig. 4 (b)).

2) The dimensionless moment is calculated as the product of force and positional vector at the cell center of the wing, such that $\boldsymbol{M} = \int_A \boldsymbol{F} \times \boldsymbol{r}\mathrm{d}A$. Here A is the wing surface area; F is the aerodynamic force in the unit wing area; $\boldsymbol{r}$ is the distance vector.

3) The translation power can be written as $\boldsymbol{P}_{\text{t}} = \int_A \boldsymbol{F} \times \boldsymbol{v}\mathrm{d}A$, and the rotation power can be written as $\boldsymbol{P}_{\text{r}} = \int_A \boldsymbol{M} \times \boldsymbol{\Omega}\mathrm{d}A$, where $\boldsymbol{v}$ is the wing velocity and $\boldsymbol{\Omega}$ is the angular velocity. The total mechanical power of the wing is $\boldsymbol{P} = \boldsymbol{P}_{\text{t}} + \boldsymbol{P}_{\text{r}}$.

3 Results and Discussion

The lift coefficient and the drag coefficient are defined as

$$C_{\text{L}} = \frac{2F_{\text{L}}}{\rho U_{\text{m}}^2 c}, \quad C_{\text{D}} = \frac{2F_{\text{D}}}{\rho U_{\text{m}}^2 c} \tag{6}$$

where C_{L}, C_{D} are the lift coefficient and the drag coefficient, respectively; ρ is the air density; U_{m} is the average velocity of the wing chord; c is the wing chord length. The aerodynamic force acting on the wing is contributed by the pressure and viscous stress on the wing surface, and the total force is the sum of pressure force and viscous force. The lift and drag refer to the total lift and total drag. Fig. 5 describes the computation results of lift coefficient C_{L} and drag coefficient C_{D}. Note that the lift coefficient and the drag coefficient are normalized and represented in the same diagram in order to compare the variation trend better. The results show that C_{L} and C_{D} have a similar variation trend with Wang's research[3]. The small difference may be due to the parameter settings and wings flexible deformation. The wing is considered to be rigid in Wang's research, while the wing is considered to be flexible in this paper.

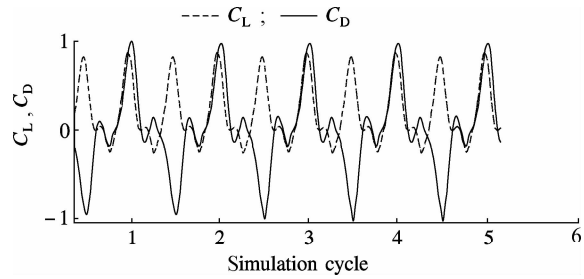

Fig. 5 Computation results of lift and drag coefficients

The negative lift and drag means that the direction of lift and drag is opposite to definition. The large lift and drag peaks at the beginning and the end of the stroke can be explained by the superposition of the rapid translational acceleration, the fast pitching-up rotation of the wing and the wing's rotation. The rotational circulation is caused by the Magnus effect, which makes the wing generate an upward force. This effect is similar to a rotational circulation mechanism[14]. Unlike the rigid wing's results[15], the small peaks before large peaks in the first quarter-cycle can be explained by the convex flow effect. The wings are rigid in the translation process, so the drag has a steady increase at this stage. Then the wing has a flexible deformation (see Fig. 4(b)①) before the rotation phase, and the wings area against airflow is reduced, so the drag has a slight decrease in this stage. The small peaks after large peaks in the second quarter-cycle can be explained by the concave flow effect, and the wings flexible deformation has not changed after the rotation phase (see Fig. 4(b)②), so the wings area against airflow is increased and the drag has a slight increase an this stage. A similar theory can be used to explain the small drag peaks in the next half flapping cycle.

The average viscous force is probably 1/400 of the pressure force and the average viscous moment is only 1/775 of the pressure moment in our computation, as shown in Fig. 6(a). The viscous force and moment can be ignored during the following insects' normal hovering flight research. The total force and the total moment can be represented by the pressure force and the pressure moment, respectively. The average rotational power is probably 1/20 of the translational power, as shown in Fig. 6(b), so insects will consume more energy for translational movement than for rotational movement. The positive power means that the flapping wings do work on fluid and the movement of wings needs to consume energy. The negative power means that the fluid produces work on flapping wings. This will help the wing form a convex flow shape and save the energy consumption of insect flight.

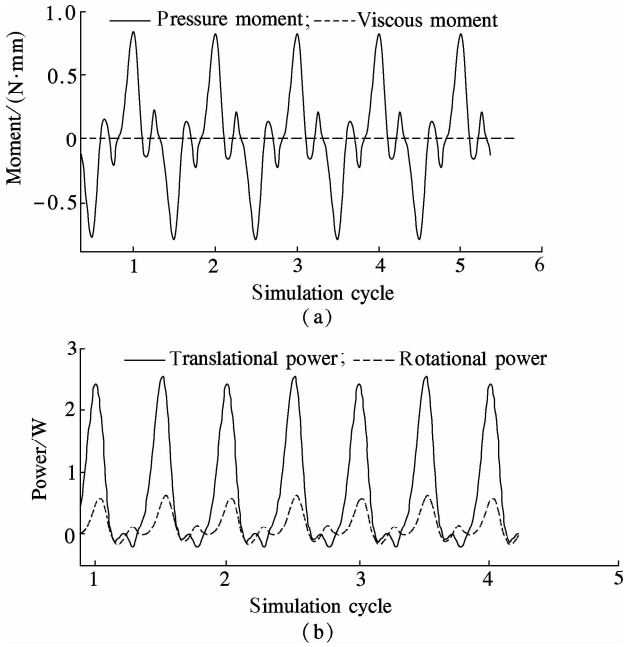

Fig. 6 Aerodynamic moment changes and consumed power during several flapping cycles. (a) Comparison between pressure moment and viscous moment; (b) Comparison between translational power and rotational power

4 Conclusion

Four insect flapping flight coordinate systems are established to represent the bees' position, attitude and wings deformation. Then the computation models of the 2-dimensional flexible wing are established, and the force, moment, and power changes are investigated. According to the computational results, the large lift and drag peaks at the beginning and end of the stroke can be explained by the superposition of the rapid translational acceleration, the fast pitching-up rotation and the Magnus effect. The small force and drag peaks can be explained by the convex flow effect and the concave flow effect. The viscous force, moment and rotational power are small and can be ignored. In the future research, a lot of work needs to be done to reveal the flight mechanism, such as numerical calculation of 3-dimensional flexible wing, quantitative analysis of force, moment and power. Understanding the mechanism of insect flight will be a great promotion of micro-flapping flight design and application.

References

[1] Ellington C P. The aerodynamics of hovering insect flight. VI. lift and power requirements[J]. *Philosophical Transactions of the Royal Society of London Series B—Biological Sciences*, 1984, **305**(1122):145 - 181.

[2] Sun Mao, Tang Jian. Lift and power requirements of hovering flight in Drosophila virilis[J]. *The Journal of Experimental Biology*, 2002, **205**(16): 2413 - 2427.

[3] Wang Z J, Birch J M, Dickinson M H. Unsteady forces and flows in low Reynolds number hovering flight: two-dimensional computations vs robotic wing experiments [J]. *The Journal of Experimental Biology*, 2004, **207**(3):449 - 460.

[4] Liu Hao. Integrated modeling of insect flight: from morphology, kinematics to aerodynamics[J]. *Journal of Computational Physics*, 2009, **228**(2): 439 - 459.

[5] Mountcastle A M, Combes S A. Wing flexibility enhances load-lifting capacity in bumblebees[J]. *Proceedings of the Royal Society of Series B—Biological Sciences*, 2013, **280**(22): 1 - 8.

[6] Tian Fangbo, Luo Haoxiang, Song Jialei, et al. Force production and asymmetric deformation of a flexible flapping wing in forward flight[J]. *Journal of Fluids and Structures*, 2013, **36**:149 - 161.

[7] Tanaka H, Whitney J P, Wood R J. Effect of flexural and torsional wing flexibility on lift generation in hoverfly flight[J]. *Integrative and Comparative Biology*, 2011, **51**(1): 142 - 150.

[8] Fry S N, Sayaman R, Dickinson M H. The aerodynamics of hovering flight in Drosophila[J]. *The Journal of Experimental Biology*, 2005, **208**(12):2303 - 2318.

[9] Wang Z J. Two dimensional mechanism for insect hovering[J]. *Physical Review Letters*, 2000, **85**(10): 2216 - 2219.

[10] Wang Z J. The role of drag in insect hovering[J]. *The Journal of Experimental Biology*, 2004, **207**(23):4147 - 4155.

[11] Sun Mao. High-lift generation and power requirements of insect flight[J]. *Fluid Dynamics Research*, 2005, **37**(1/2):21 - 39.

[12] Wang Z J. Computation of insect hovering[J]. *Mathematical Methods in the Applied Sciences*, 2001, **24**(17/18):1515 - 1521.

[13] Lu Guang, Yan Jingping, Zhang Zhisheng, et al. Dissection of a flexible wing's performance for insect-inspired flapping-wing micro air vehicles[J]. *Advanced Robotics*, 2012, **26**(5/6): 409 - 435.

[14] Dickinson M H, Lehmann F O, Sane S. Wing rotation and the aerodynamic basis of insect flight[J]. *Science*, 1999, **284**(5422):1954 - 1960.

[15] Zhang Genbao, Liu Yijun, Shi Wu, et al. Numerical simulation of two-dimensional flapping-wing MAVs[J]. *Journal of Donghua University: Natural Science*, 2011, **37**(2): 256 - 260. (in Chinese)

蜜蜂悬停飞行时柔性翅气动特性

尹东富　张志胜

（东南大学机械工程学院，南京 211189）

摘要：对蜜蜂悬停飞行时二维柔性翅气动特性进行了研究. 建立了昆虫飞行的 4 种坐标系，包括地面坐标系、贴体坐标系、固定翼坐标系和柔性翼坐标系，分别表示昆虫的位置、姿态、翅膀运动形式及变形. 对 4 种坐标系间的变换进行了研究，并指出在二维刚性翅研究中利用椭圆坐标系可以提高计算精度，减少计算量. 建立了二维柔性翅模型，分析了气动力、力矩及功率变化情况. 对计算结果进行了分析，并指出扑动开始及结束阶段大的升力和阻力峰值的产生是平动加速、加速旋转及马格纳斯效应的叠加；小的峰值归因于凸向来流和凹向来流作用；与压力、压力力矩和平动功率相比，黏性力、黏性力矩及转动功率较小，可以忽略.

关键词：扑翼；坐标系；悬停飞行；计算流体动力学；气动力；功率

中图分类号：V211. 3